WATER RESOURCES RESEARCH, VOL. 36, NO. 1, PAGES 173–179, JANUARY 2000

Virus transport in unsaturated porous media

Youn Sim and Constantinos V. Chrysikopoulos

Department of Civil and Environmental Engineering, University of California, Irvine

Abstract. A numerical model for one-dimensional virus transport in homogeneous, unsaturated porous media was developed. The model accounts for virus sorption onto liquid-solid and air-liquid interfaces as well as inactivation of viruses suspended in the liquid phase and viruses attached at both interfaces. The effects of the moisture content variation on virus transport in unsaturated porous media were investigated. In agreement with previous experimental studies, model simulations indicated that virus sorption is greater at air-liquid than liquid-solid interfaces. Available data from experiments of colloid transport through unsaturated columns were successfully simulated by the virus transport model developed in this study.

1. Introduction

Most of the common viruses present in the subsurface originate from human and animal sewage through wastewater discharges, sanitary landfills, septic tanks, and agricultural practices. Experimental studies revealed that viruses survive a considerable period of time in unsaturated porous media before they reach the water table [*Schaub and Sorber*, 1977]. Therefore it is important to understand fully the mechanisms governing the transport and fate of these microorganisms in unsaturated porous media.

Virus transport in unsaturated porous media is distinguished from transport in saturated porous media, because virus sorption and inactivation are considerably influenced by the soil moisture content and subsurface temperature fluctuations [*Vilker and Burge*, 1980; *Vilker*, 1981; *Thompson and Yates*, 1999]. Unsaturated porous media consist of liquid, solid, and air phases. For water-wet solid surfaces, both liquid-solid and air-liquid interfaces exist. Virus sorption within unsaturated porous media is significantly affected by the presence of these two interfaces. An illustration of the three phases present in unsaturated porous media together with viruses in the liquid phase and at the associated two interfaces is shown in Figure 1.

Although viruses may undergo sorption onto liquid-solid interfaces via physical adsorption, chemical sorption, or ion exchange, virus sorption onto liquid-solid interfaces mainly results from electrostatic double-layer interactions and van der Waals forces [*Teutsch et al*., 1991]. It should be noted that virus sorption behavior evaluated from batch studies is not consistent with results from column or field experiments [*Powelson and Gerba*, 1994]. However, *Jin et al*. [1997] indicated that virus sorption is determined more effectively with a well-controlled column flow system. Furthermore, *Vilker* [1981] suggested that nonequilibrium kinetic sorption is appropriate for models describing virus attachment onto liquid-solid interfaces and for viruses with size relatively small or similar to the size of solutes. This sorption process represents the rate of approach to equilibrium between adsorbed and liquid phase virus concentrations, accounting for virus transport to the outer layer of a solid particle by mass transfer, followed by virus immobilization.

Numerous investigations suggest that virus sorption is strongly correlated with the degree of soil moisture. *Lance et al*. [1976] and *Lance and Gerba* [1984] reported that decreasing the moisture content enhances virus sorption onto the solid matrix by forcing viruses to move into a thin film of water surrounding soil particles. However, *Powelson et al*. [1990, 1991] and *Poletika et al*. [1995] indicated that the enhanced removal of viruses at low soil moisture content is due to the sorption of viruses onto air-liquid interfaces in addition to virus sorption onto liquid-solid interfaces. *Wan and Wilson* [1994a, b] also experimentally demonstrated that colloids such as viruses strongly adsorb onto air-liquid interfaces. *Powelson et al*. [1990] suggested that virus sorption is greater at air-liquid than liquid-solid interfaces.

Virus sorption at air-liquid interfaces is mainly controlled by virus particle surface hydrophobicity, solution ionic strength, and particle charge [*Wan and Wilson*, 1994a]. The primary forces controlling virus sorption at air-liquid interfaces are van der Waals and interactions between hydrophobic groups on viruses and solid surfaces. Virus sorption at an air-liquid interface is essentially irreversible because of the strong binding exerted by capillary forces. Consequently, viruses at an air-liquid interface may be desorbed only under high interfacial shear stresses induced by fast interstitial fluid flow [*Wan and Wilson*, 1994a; *Poletika et al*., 1995]. Virus sorption onto air-liquid interfaces in unsaturated porous media is governed by temporal and spatial variations of the moisture content; however, the nonlinear relationship between moisture content and virus sorption at air-liquid interfaces is not well understood.

Virus inactivation is defined as a loss of viral titer with time due to disruption of coat proteins and degradation of nucleic acid [*Gerba*, 1984]. Virus inactivation is controlled by many factors, including temperature, microbial activity, moisture content, pH, and soil properties, to mention a few [*Yates and Yates*, 1988]. Virus inactivation is often considered as a first-order irreversible sink mechanism [*Yates and Yates*, 1988; *Sim and Chrysikopoulos*, 1996]. The inactivation rate coefficient is smaller for viruses attached at a liquid-solid interface than viruses suspended in the liquid phase [*Hurst et al*., 1980; *Vilker*, 1981; *Gerba*, 1984; *Yates and Yates*, 1988]. Consequently, recent mathematical models for virus transport in saturated porous media account for different inactivation rates for viruses in different phases [*Chrysikopoulos and Sim*, 1996; *Sim and Chrysikopoulos*, 1995, 1998].

Viruses sorbed at air-liquid interfaces undergo enhanced

Paper number 1999WR900302.
0043-1397/00/1999WR900302$09.00

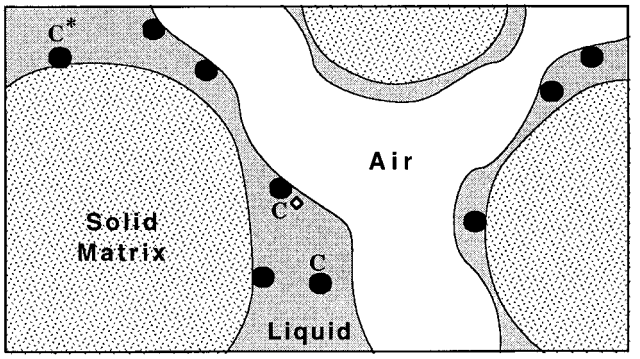

Figure 1. Schematic illustration of viruses distributed in an unsaturated porous medium, where C represents viruses in the liquid phase, C^* viruses sorbed at liquid-solid interface, and $C^\diamond$ viruses sorbed at air-liquid interface.

inactivation [*Thompson et al*., 1998]. When a fluid (i.e., water) is in contact with another immiscible fluid (i.e., air), the difference between the inward attraction of the molecules within each immiscible fluid and those at the interface of the two fluids leads to interfacial tension [*Bear*, 1972, p. 441]. Thus, for viruses sorbed at air-liquid interfaces, the interfacial tension along the virus particles creates a deforming force, which results in disruption of coat proteins and consequently promotes virus inactivation [*Trouwborst et al*., 1974].

Only a few mathematical models are available in the literature describing virus transport in unsaturated porous media. These models employ invariant virus sorption and inactivation parameters and do not account for the effect of soil moisture content variation on virus sorption at liquid-solid and air-liquid interfaces. *Tim and Mostaghimi* [1991] developed a numerical model for water flow and virus transport in variably saturated formations assuming that virus sorption is an equilibrium process and that the virus inactivation rate is identical for adsorbed as well as liquid phase viruses. *Park et al*. [1992] developed a semianalytical/numerical model (Viralt) for both steady state and transient vertical virus transport in the unsaturated zone and along the flow lines in the saturated zone, accounting for equilibrium sorption and first-order inactivation. *Yates and Ouyang* [1992] developed a one-dimensional numerical model (Virtus) that couples the flow of water, viruses, and heat in unsaturated porous media accounting for moisture-independent sorption, filtration, and temperature-dependent inactivation.

This work provides a mathematical model for virus transport in one-dimensional, homogeneous, unsaturated porous formations. Virus sorption onto liquid-solid as well as air-liquid interfaces is accounted for. Furthermore, inactivation of viruses suspended in the liquid phase and viruses attached at both interfaces are incorporated into the transport model. The effect of moisture content variation on virus transport in unsaturated porous media is investigated. The model is applied to available experimental data.

2. Model Development

2.1. Virus Transport

The vertical virus transport in one-dimensional, unsaturated porous media accounting for virus sorption and inactivation is governed by the following partial differential equation:

$$\frac{\partial}{\partial t}[\theta_m C] + \rho \frac{\partial C^*}{\partial t} + \frac{\partial}{\partial t}[\theta_m C^\diamond] = \frac{\partial}{\partial z}\left[D_z \theta_m \frac{\partial C}{\partial z}\right] - \frac{\partial}{\partial z}[qC] - \lambda \theta_m C - \lambda^* \rho C^* - \lambda^\diamond \theta_m C^\diamond, \quad (1)$$

where $C(t, z)$ is the virus concentration in the liquid phase; $C^*(t, z)$ is the adsorbed virus concentration at the liquid-solid interface; $C^\diamond(t, z)$ is the adsorbed virus concentration at the air-liquid interface; q is the specific discharge (Darcian fluid flux); θ_m is the moisture content (moisture volume divided by the total volume of the porous medium); λ, λ^*, and $\lambda^\diamond$ are the inactivation rate coefficients of viruses in the liquid phase, viruses sorbed at the liquid-solid interface, and viruses sorbed at the air-liquid interface, respectively; ρ is the bulk density of the solid matrix; t is time; and z is the spatial coordinate in the vertical direction (z increases in the downward direction). The last three terms on the right-hand side of (1) represent the inactivation of liquid phase viruses, viruses sorbed at the liquid-solid interface, and viruses sorbed at the air-liquid interface, respectively. Furthermore, the second and third terms on the left-hand side of (1) represent virus accumulation at the liquid-solid and air-liquid interfaces, respectively. The vertical hydrodynamic dispersion coefficient D_z is defined as [*Nielsen et al*., 1986]

$$D_z = \alpha_z \frac{q}{\theta_m} + \mathcal{D}_e, \quad (2)$$

where $\mathcal{D}_e = \mathcal{D}/\tau$ is the effective molecular diffusion coefficient in the unsaturated porous medium (where $\mathcal{D}$ is the molecular diffusion coefficient and $\tau \geq 1$ is the tortuosity coefficient) and α_z is the vertical dispersivity.

The virus inactivation rate coefficients λ, λ^*, and $\lambda^\diamond$ are time- and temperature-dependent [*Sim and Chrysikopoulos*, 1996]; however, in this study they are assumed to be constant. Furthermore, *Yates and Ouyang* [1992] suggested that the inactivation rate coefficients of viruses sorbed onto a liquid-solid interface are approximately one half of the coefficients for liquid phase viruses ($\lambda^* = \lambda/2$) owing to the protective effect of the solid matrix. Although virus sorption at the air-water interface enhances virus inactivation [*Thompson et al*., 1998], there is no quantitative relationship between λ and $\lambda^\diamond$ available in the literature. Consequently, in the present study it is assumed that $\lambda^\diamond = \lambda$.

The initial and boundary conditions for the transport system examined here are

$$C(0, z) = C^*(0, z) = C^\diamond(0, z) = 0, \quad (3)$$

$$-D_z \theta_m \frac{\partial C(t, 0)}{\partial z} + q(t, 0)C(t, 0) = \begin{cases} q(t, 0)C_0 & 0 \leq t \leq t_p \\ 0 & t_p < t \end{cases} \quad (4)$$

$$\frac{\partial C(t, \infty)}{\partial z} = 0, \quad (5)$$

where C_0 is the pulse-type source concentration and t_p is the duration of the pulse. The condition (3) establishes that there is no initial liquid phase and adsorbed virus concentrations within the porous medium. The flux-type boundary condition (4) for pulse injection implies concentration discontinuity at the ground surface (inlet) and leads to material balance con-

servation [*Parker and van Genuchten*, 1984; *Chrysikopoulos et al*., 1990a, b]. The downstream boundary condition (5) preserves concentration continuity for a vertical, semi-infinite porous medium.

2.2. Virus Sorption Onto Interfaces

The accumulation of deposited viruses at solid-liquid and air-liquid interfaces is described by the following expressions [*Sim and Chrysikopoulos*, 1999]:

$$\rho \frac{\partial C^*}{\partial t} = k\theta_m(C - C_g) - \lambda^* \rho C^* \tag{6}$$

$$\frac{\partial}{\partial t}(\theta_m C^{\diamond}) = k^{\diamond}\theta_m C - \lambda^{\diamond}\theta_m C^{\diamond}, \tag{7}$$

where k and $k^{\diamond}$ are the liquid to liquid-solid and liquid to air-liquid interface mass transfer rates, respectively, and $C_g(t, z)$ is the liquid phase concentration of viruses in direct contact with solids. It is assumed that the following linear equilibrium relationship is valid [*Sim and Chrysikopoulos*, 1996]:

$$C^* = K_d C_g, \tag{8}$$

where K_d is the partition or distribution coefficient. Furthermore, the liquid to liquid-solid interface mass transfer rate is expressed as

$$k = \kappa a_T, \tag{9}$$

where κ is the liquid to liquid-solid interface mass transfer coefficient and a_T is the specific liquid-solid interface area, defined as the ratio of total surface area of soil particles to the bulk volume of the porous medium [*Fogler*, 1992]

$$a_T = \frac{3(1 - \theta_s)}{r_p}, \tag{10}$$

where r_p represents the average radius of soil particles and θ_s is the water content of a saturated porous medium. It should be noted that the transfer of viruses from the bulk liquid to a liquid-solid interface is assumed to be governed by virus diffusion through an outer liquid layer surrounding the soil particle. The thickness of this liquid layer depends on local hydrodynamic conditions [*Vilker and Burge*, 1980; *Fogler*, 1992]. Virus sorption onto solids occurs if the liquid phase virus concentration (C) is greater than liquid phase virus concentration in direct contact with solids (C_g), whereas desorption occurs when C is smaller than C_g.

The liquid to air-liquid interface mass transfer rate is defined as

$$k^{\diamond} = \kappa^{\diamond} a_T^{\diamond}, \tag{11}$$

where $\kappa^{\diamond}$ is the liquid to air-liquid interface mass transfer coefficient and $a_T^{\diamond}$ is the specific air-liquid interface area, defined as the ratio of the total air-liquid interface area to the bulk volume of the porous medium [*Cary*, 1994]

$$a_T^{\diamond}(\theta_m) = \frac{2\theta_s^b}{r_0}\left(\zeta\theta_r \frac{\theta_s^{-b} - \theta_m^{-b}}{-b} + \frac{\theta_s^{1-b} - \theta_m^{1-b}}{1-b}\right), \tag{12}$$

where ζ and b are empirical, soil type specific constants; θ_r is the residual or monolayer moisture content; and r_0 is the effective pore radius at air entry which can be evaluated by the capillary rise equation with zero contact angle as follows [*Guymon*, 1994, p. 43]:

$$r_0 = \frac{2\sigma}{\rho_w g h_0}, \tag{13}$$

where σ is the surface tension of water; ρ_w is the density of water; g is the gravitational constant; and h_0 is the air-entry value, defined as the pore water head where air begins to enter water-saturated pores [*Guymon*, 1994]. Note that $a_T^{\diamond}$ is a function of moisture content and takes a zero value when $\theta_m = \theta_s$. Thus (11) and (12) suggest that the liquid to air-liquid interface mass transfer rate $k^{\diamond}$ decreases with increasing moisture content. Consequently, the transfer of viruses at the air-liquid interface is controlled by the moisture content level. Furthermore, it should be noted that for a given moisture content the accumulation of viruses at air-liquid interfaces, as described by (7), is governed by irreversible virus sorption onto the air-water interface and subsequent virus inactivation. Therefore the model presented in this work implicitly assumes that the timescale associated with aquifer saturation due to progressive increase in moisture content (rewetting) is substantially larger than the timescale associated with complete virus inactivation. Consequently, viruses previously sorbed at air-water interfaces are not expected to partition back into the liquid phase.

2.3. Variably Saturated Flow

The one-dimensional water infiltration into effectively semi-infinite, homogeneous, unsaturated, rigid porous media is described by the following nonlinear equation which is a modified form of the Richards equation [*Philip*, 1969; *Bear*, 1972, p. 511]:

$$\frac{\partial \theta_m(\psi)}{\partial \psi}\frac{\partial \psi}{\partial t} = \frac{\partial}{\partial z}\left(K(\psi)\frac{\partial \psi}{\partial z}\right) - \frac{\partial K(\psi)}{\partial z}, \tag{14}$$

where ψ is the pressure head potential and $K(\psi)$ is the unsaturated hydraulic conductivity. The preceding equation neglects possible effects on variably saturated flow due to the presence of air and perhaps any thermal gradients. Several empirical functions are available in the literature for the estimation of the unsaturated hydraulic conductivity; however, the relationship developed by *van Genuchten* [1980] based on the predictive conductivity model of *Mualem* [1976] is employed here:

$$K(\psi) = K_s S_e^{1/2}[1 - (1 - S_e^{1/\eta})^{\eta}]^2, \tag{15}$$

where K_s is the saturated hydraulic conductivity and S_e is the effective saturation defined as

$$S_e = \frac{\theta_m - \theta_r}{\theta_s - \theta_r}, \tag{16}$$

where the moisture content θ_m and its derivative with respect to ψ are determined by

$$\theta_m(\psi) = \theta_r + \frac{\theta_s - \theta_r}{(1 + |\alpha\psi|^{\beta})^{\eta}}, \tag{17}$$

$$\frac{d\theta_m}{d\psi} = -\eta(1 + |\alpha\psi|^{\beta})^{-\eta-1}\beta\alpha|\alpha\psi|^{\beta-1}(\theta_s - \theta_r), \tag{18}$$

respectively, where α, β, and $\eta = 1 - 1/\beta$ are empirical coefficients. For example, $\alpha = 0.0547$ cm^{-1}, $\beta = 4.26$, and $\eta = 0.765$ for Dune sand [*Gillham et al*., 1979].

The initial and boundary conditions used for the variably saturated flow system are

$$\psi(0, z) = \psi_i, \tag{19}$$

Table 1. Model Parameters for Simulations

Parameter	Value	Reference
b	2	*Cary* [1994]
$\mathcal{D}_e$	1.542×10^{-5} cm^2 h^{-1}	*Tim and Mostaghimi* [1991]
g	980 cm s^{-2}	
h_0	2 cm	*Cary* [1994]
K_d	20 cm^3 g^{-1}	*Vilker and Burge* [1980]
r_p	0.1 cm	*Vilker and Burge* [1980]
α_z	0.5 cm	*Domenico and Schwartz* [1990]
ζ	160	*Cary* [1994]
θ_s	0.45	*Cary* [1994]
κ	0.006 cm h^{-1}	*Vilker and Burge* [1980]
ρ	1.5 g cm^{-3}	*Yates and Ouyang* [1992]
σ	74.2×10^{-3} N m^{-1}	*Guymon* [1994]

$$\left(-K\frac{\partial\psi}{\partial z}+K\right)\Big|_{z=0}=q_0, \tag{20}$$

$$\frac{\partial\psi(t,\infty)}{\partial z}=0, \tag{21}$$

where ψ_i is the initial pressure head potential and q_0 is the prescribed net specific discharge (positive flux corresponds to downward flow). Condition (19) indicates that the initial pressure head potential is uniformly distributed within the porous medium. Condition (20) signifies that the water flux at the ground surface is prescribed, whereas condition (21) implies a free draining bottom boundary. It should be noted that the specific discharge (Darcian fluid flux) is defined as $q = -K(\partial\psi/\partial z - 1)$.

The governing equations for virus transport (1) and variably saturated flow (14) in conjunction with the relationships (6)–(13) and (15)–(18) are solved numerically subject to initial/boundary conditions (3)–(5) and (19)–(21). The numerical solutions are obtained by using appropriate *International Mathematics and Statistics Libraries, Inc*. [1991] one-dimensional partial differential equation solvers.

3. Model Simulations

In order to illustrate the effect of moisture content variation on virus fate and transport in unsaturated porous media, model simulations are performed for a variety of situations. Because appropriate values for $\kappa^{\diamond}$ are not available in the literature, it is assumed that $\kappa^{\diamond} = 5\kappa$. This assumption is based on experimental observations suggesting that colloid particles are sorbed more strongly onto air-liquid interfaces than onto liquid-solid interfaces [*Wan and Wilson*, 1994a]. Unless specified otherwise, all fixed model parameter values used for model simulations are listed in Table 1. The values for the empirical coefficients ζ, b, h_0, and θ_r for sand are adopted from *Cary* [1994]. All virus concentrations are conveniently normalized by the source concentration.

For the special case of a one-dimensional, homogeneous aquifer with uniform moisture content and negligible virus inactivation, model-predicted virus concentration breakthrough curves and snapshots are presented in Figures 2a and 2b, respectively. Three different aquifer moisture content levels are examined. The case of $\theta_m = 0.45$ represents the case of complete water saturation. Clearly, Figure 2 indicates that decreasing the aquifer moisture content from complete saturation to partial saturation leads to a substantial reduction in the liquid phase virus concentration. This is attributed to the increased virus transfer from the liquid phase to the air-liquid interface caused by the decrease in moisture content as described by relationships (11) and (12).

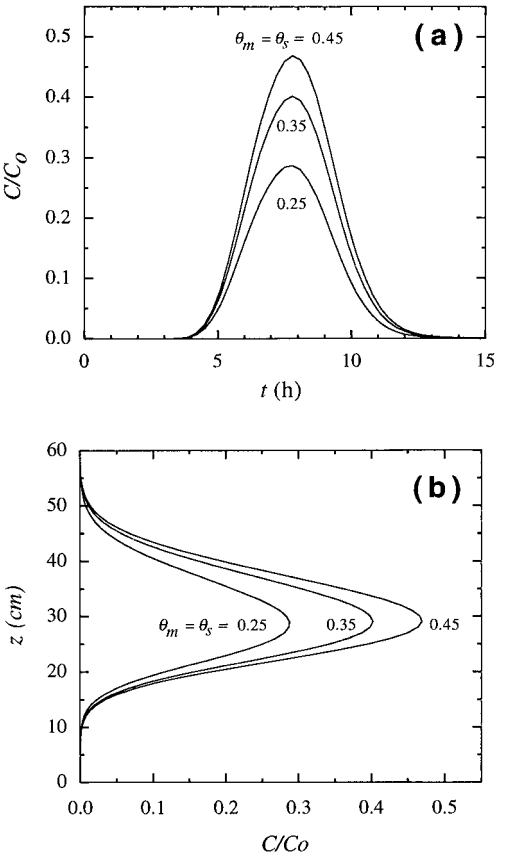

Figure 2. Normalized liquid phase virus distributions for various moisture content levels as a function of (a) time and (b) vertical distance ($t = 8$ hours, $x = 30$ cm, $t_p = 3.3$ hours, $U = 4.8$ cm h^{-1}, $\kappa^{\diamond} = 5\kappa$, and $\lambda = \lambda^* = \lambda^{\diamond} = 0$).

4. Comparison With Experimental Data

The virus transport model presented is employed to simulate the hydrophilic colloid breakthrough response from two column experiments published by *Wan and Wilson* [1994b]. Two different water saturation levels (54% and 100%) were examined. It should be noted that despite the different water saturations both experiments were conducted under the same constant interstitial velocity ($U = q/\theta_m = 10$ cm h^{-1}). Consequently, q and D_z are constant parameters. Furthermore, the column experiments were conducted under the same conditions, and identical colloid particles were used. For the case of 100% saturation ($\theta_m = \theta_s = 0.43$), given the values of r_p, U, θ_s, and ρ listed in Table 2, a nonlinear least squares regression method [*IMSL*, 1991] was employed for the estimation of the unknown parameters D_z, k, and K_d by fitting the virus transport model to the observed colloid concentrations. The parameter $k^{\diamond}$ was set to zero because at 100% water saturation there are no air-liquid interfaces present. The parameter κ was calculated by (9) with a value for a_T estimated by (10). The desired parameter values together with the corresponding residual sum of squared error (SSE) and correla-

Table 2. Estimated and Calculated Parameters Corresponding to the Experimental Data

Parameter	100% Water Saturation ($\theta_m = \theta_s = 0.430$)	54% Water Saturation ($\theta_m = 0.232$)
	Experimental Parameters [Wan and Wilson, *1994b*]	
r_p	212 to ~315 μm (average 263.5 μm)	212 to ~315 μm (average 263.5 μm)
U	10 cm h^{-1}	10 cm h^{-1}
θ_s	0.43	0.43
ρ	1.65 g cm^{-3}	1.65 g cm^{-3}
	Estimated Parameters	
D_z	2.81 cm^2 h^{-1}	...
k	0.0282 $hour^{-1}$	0.0282 $hour^{-1}$
K_d	52.73 cm^3 g^{-1}	48.55 cm^3 g^{-1}
$k^{\diamond}$	...	0.0751 $hour^{-1}$
SSE	0.02748	0.02882
CC	0.993	0.989
	Calculated Parameters	
a_T	65.8 cm^{-1}	65.8 cm^{-1}
$a_T^{\diamond}$	...	28.74 cm^{-1}
κ	0.000428 cm h^{-1}	0.000428 cm h^{-1}
$\kappa^{\diamond}$	...	0.00261 cm h^{-1}

SSE is sum of squared error; CC is correlation coefficient.

tion coefficient (CC) are listed in Table 2. Figure 3 clearly shows a good agreement between the model simulation (solid curve) and the experimental data (circles) for the 100% saturation case.

For the 54% saturation case ($\theta_m = 0.232$) the only unknown parameters are k, K_d, and $k^{\diamond}$, because D_z is essentially the same as for the 100% saturation case. The parameter κ was calculated by (9) with a value for a_T estimated by (10). It is interesting to note that the calculated value for κ (κ = 0.000428 cm h^{-1}, see Table 2) is exactly the same for both water saturation cases considered here. This result is expected because both experiments were conducted under the same interstitial velocity U and chemical conditions with identical colloid particles. Apparently, these are the factors controlling the liquid to liquid-solid interface mass transfer coefficient κ [*Vilker and Burge*, 1980; *Fogler*, 1992]. The parameter $\kappa^{\diamond}$ was calculated from the estimated value of $k^{\diamond}$ by employing (11) with $a_T^{\diamond}$ as estimated by (12) with necessary values for b, h_0, ζ, and θ_r obtained from the work by *Cary* [1994], assuming that the column packing material used by *Wan and Wilson* [1994b] was similar to sand with $r_p \simeq 263.5$ μm. The parameter values for the 54% saturation case together with the corresponding SSE and CC are also listed in Table 2. Overall, good agreement between the model simulation (dashed line) and the experimental data (squares) for the 54% saturation case is shown in Figure 3. It should be noted that the model underestimated slightly the small tail of the experimental breakthrough data ($t \geq 7.5$ hours). The difference between the simulated concentration history and experimental data is within the experimental error calculated by *Wan and Wilson* [1994b] but does not necessarily exclude the possibility of inaccurate model prediction of colloid desorption. The calculated value of $\kappa^{\diamond}$ is approximately 6 times larger than the one for κ, because the air-liquid interface serves as a stronger adsorbent than the liquid-solid interface, as suggested by available experimental studies [e.g., *Wan and Wilson*, 1994a]. Moreover, this result is quite consistent with our initial assumption that $\kappa^{\diamond} = 5\kappa$, employed for the model simulations presented in Figure 2.

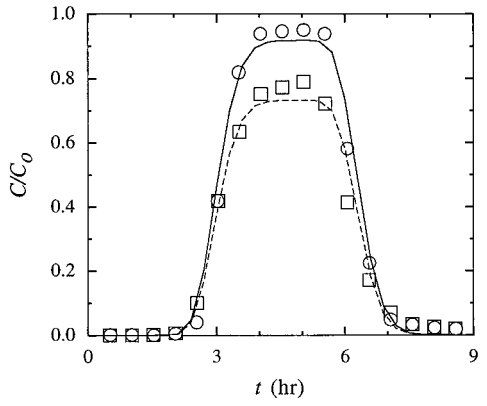

Figure 3. Normalized concentrations of hydrophilic colloid breakthrough data (symbols) adopted from *Wan and Wilson* [1994b] and simulated concentration histories (curves). Squares and dashed curve represent experimental data and model simulation, respectively, at 54% water saturation, whereas circles and solid curve represent data and model simulation, respectively, at 100% water saturation.

5. Summary

A numerical virus transport model is developed to investigate the effects of moisture content variation on virus transport in one-dimensional, homogeneous, unsaturated porous media. The model accounts for moisture-controlled virus sorption onto the liquid-solid as well as air-liquid interfaces and virus inactivation in the liquid phase and at the interfaces. Model simulations indicate that virus transport in unsaturated porous media is highly sensitive to interstitial moisture variability. At low moisture content levels the transport of viruses is significantly affected by the irreversible sorption of viruses onto air-liquid interfaces. The virus transport model developed here was used to successfully fit existing experimental data. In agreement with previous experimental investigations published in the literature, the results from this fitting exercise indicate that the liquid to air-liquid interface colloid transfer is greater than the liquid to air-liquid interface transfer.

Notation

a_T specific liquid-solid interface area, $L^2\ L^{-3}$.
$a_T^{\diamond}$ specific air-liquid interface area, $L^2\ L^{-3}$.
b empirical constant.
C concentration of viruses in suspension (liquid phase), $M\ L^{-3}$.
C_0 source concentration, $M\ L^{-3}$.
C^* deposited virus concentration at the liquid-solid interface (virus mass/solids mass), $M\ M^{-1}$.
$C^{\diamond}$ adsorbed virus concentration at the air-liquid interface, $M\ L^{-3}$.
C_g concentration of viruses directly in contact with solids, $M\ L^{-3}$.
$\mathcal{D}$ molecular diffusion coefficient, $L^2\ t^{-1}$.
$\mathcal{D}_e$ effective molecular diffusion coefficient, $L^2\ t^{-1}$.
D_z vertical hydrodynamic dispersion coefficient, $L^2\ t^{-1}$.
g gravitational constant, $L\ t^{-2}$.
h_0 air-entry value, L.
k liquid to liquid-solid interface mass transfer rate, t^{-1}.
$k^{\diamond}$ liquid to air-liquid interface mass transfer rate, t^{-1}.
K unsaturated hydraulic conductivity, $L\ t^{-1}$.
K_d partition or distribution coefficient, $L^3\ M^{-1}$.
K_s saturated hydraulic conductivity, $L\ t^{-1}$.
q specific discharge (Darcian fluid flux), $L\ t^{-1}$.
q_0 prescribed specific discharge, $L\ t^{-1}$.
r_0 effective pore radius at air entry, L.
r_p average radius of soil particles, L.
S_e effective saturation coefficient, defined in (16).
t time.
t_p duration of source pulse, t.
U average interstitial velocity ($U = q/\theta_m$), $L\ t^{-1}$.
z spatial coordinate in vertical direction, L.

α empirical coefficient, L^{-1}.
α_z vertical dispersivity, $L\ t^{-1}$.
β empirical coefficient.
ζ empirical coefficient.
η empirical coefficient, equal to $1 - 1/\beta$.
θ_m moisture content (liquid volume/porous medium volume), $L^3\ L^{-3}$.
θ_r residual volumetric moisture content, $L^3\ L^{-3}$.
θ_s volumetric water content of a saturated porous medium, $L^3\ L^{-3}$.
κ liquid to liquid-solid interface mass transfer coefficient, $L\ t^{-1}$.
$\kappa^{\diamond}$ liquid to air-liquid interface mass transfer coefficient, $L\ t^{-1}$.
λ inactivation rate coefficient of liquid phase viruses, t^{-1}.
λ^* inactivation rate coefficient of sorbed viruses at the liquid-solid interface, t^{-1}.
$\lambda^{\diamond}$ inactivation rate coefficient of sorbed viruses at the air-liquid interface, t^{-1}.
ρ bulk density of the solid matrix (solids mass/aquifer volume), $M\ L^{-3}$.
σ surface tension of water, $M\ t^{-2}$.
τ tortuosity ($\tau \geq 1$).
ψ pressure head potential, L.
ψ_i initial pressure head potential, L.

Acknowledgments. This work was sponsored by the National Water Research Institute and the University of California Water Resources Center as part of Water Resources Center Project W-890. The content of this manuscript does not necessarily reflect the views of the agencies, and no official endorsement should be inferred.

References

Bear, J., *Dynamics of Fluids in Porous Media*, Dover, Mineola, N. Y., 1972.
Cary, J. W., Estimating the surface area of fluid phase interfaces in porous media, *J. Contam. Hydrol.*, *15*, 243–248, 1994.
Chrysikopoulos, C. V., and Y. Sim, One-dimensional virus transport in homogeneous porous media with time dependent distribution coefficient, *J. Hydrol.*, *185*, 199–219, 1996.
Chrysikopoulos, C. V., P. K. Kitanidis, and P. V. Roberts, Analysis of one-dimensional solute transport through porous media with spatially variable retardation factor, *Water Resour. Res.*, *26*(3), 437–446, 1990a.
Chrysikopoulos, C. V., P. V. Roberts, and P. K. Kitanidis, One-dimensional solute transport in porous media with partial well-to-well recirculation: Application to field experiments, *Water Resour. Res.*, *26*(6), 1189–1195, 1990b.
Domenico, P. A., and F. W. Schwartz, *Physical and Chemical Hydrogeology*, 824 pp., John Wiley, New York, 1990.
Fogler, H. S., *Elements of Chemical Reaction Engineering*, 2nd ed., Prentice-Hall, Englewood Cliffs, N. J., 1992.
Gerba, C. P., Applied and theoretical aspects of virus adsorption to surfaces, *Adv. Appl. Microbiol.*, *30*, 133–168, 1984.
Gillham, R. W., A. Klute, and D. F. Heermann, Measurement and numerical simulation of hysteritic flow in a heterogeneous porous medium, *Soil Sci. Soc. Am. J.*, *43*(6), 1061–1067, 1979.
Guymon, G. L., *Unsaturated Zone Hydrology*, Prentice-Hall, Englewood Cliffs, N. J., 1994.
Hurst, C. J., C. P. Gerba, and I. Cech, Effects of environmental variables and soil characteristics on virus survival in soil, *Appl. Environ. Microbiol.*, *40*, 1067–1079, 1980.
International Mathematics and Statistics Libraries, Inc., *IMSL MATH/LIBRARY User's Manual*, ver. 2.0, Houston, Tex., 1991.
Jin, Y., M. V. Yates, S. S. Thompson, and W. A. Jury, Sorption of viruses during flow through saturated sand columns, *Environ. Sci. Technol.*, *31*(2), 548–555, 1997.
Lance, J. C., and C. P. Gerba, Virus movement in soil during saturated and unsaturated flow, *Appl. Environ. Microbiol.*, *47*, 335–337, 1984.
Lance, J. C., C. P. Gerba, and J. L. Melnick, Virus movement in soil columns flooded with secondary sewage effluent, *Appl. Environ. Microbiol.*, *32*, 520–526, 1976.
Mualem, Y., A new model for predicting the hydraulic conductivity of unsaturated media, *Water Resour. Res.*, *12*(3), 513–522, 1976.
Nielsen, D. R., M. T. van Genuchten, and J. W. Biggar, Water flow and solute transport processes in the unsaturated zone, *Water Resour. Res.*, *22*(9), 89S–108S, 1986.
Park, N., T. N. Blanford, and P. S. Huyakorn, VIRALT: A modular semi-analytical and numerical model for simulating viral transport in ground water, *Rep. FOS 408*, Int. Ground Water Model. Cent., Colo. Sch. of Mines, Golden, 1992.
Parker, J. C., and M. T. van Genuchten, Flux-averaged and volume-averaged concentrations in continuum approaches to solute transport, *Water Resour. Res.*, *20*(7), 866–872, 1984.
Philip, J. R., The theory of infiltration, in *Advances in Hydroscience*, vol. 5, edited by V. T. Chow, pp. 215–296, Academic, San Diego, Calif., 1969.
Poletika, N. N., W. A. Jury, and M. V. Yates, Transport of bromide, simazine, and MS-2 coliphage in a lysimeter containing undisturbed, unsaturated soil, *Water Resour. Res.*, *31*(4), 801–810, 1995.
Powelson, D. K., and C. P. Gerba, Virus removal from sewage effluents during saturated and unsaturated flow through soil columns, *Water Resour.*, *28*, 2175–2181, 1994.
Powelson, D. K., J. R. Simpson, and C. P. Gerba, Virus transport and survival in saturated and unsaturated flow through soil columns, *J. Environ. Qual.*, *19*, 396–401, 1990.
Powelson, D. K., J. R. Simpson, and C. P. Gerba, Effects of organic matter on virus transport in unsaturated flow, *Appl. Environ. Microbiol.*, *57*, 2192–2196, 1991.
Schaub, S. A., and C. A. Sorber, Virus and bacteria removal from wastewater by rapid infiltration through soil, *Appl. Environ. Microbiol.*, *33*, 609–619, 1977.
Sim, Y., and C. V. Chrysikopoulos, Analytical models for one-dimensional virus transport in saturated porous media, *Water Re-*

sour. Res., *31*(5), 1429–1437, 1995. (Correction, *Water Resour. Res*., *32*(5), 1473, 1996.)

Sim, Y., and C. V. Chrysikopoulos, One-dimensional virus transport in porous media with time-dependent inactivation rate coefficients, *Water Resour. Res*., *32*(8), 2607–2611, 1996.

Sim, Y., and C. V. Chrysikopoulos, Three-dimensional analytical models for virus transport in saturated porous media, *Transp. Porous Media*, *30*(1), 87–112, 1998.

Sim, Y., and C. V. Chrysikopoulos, Analytical models for virus adsorption and inactivation in unsaturated porous media, *Colloids Surf. A*, *155*, 189–197, 1999.

Teutsch, G., K. Herbold-Paschke, D. Tougianidou, T. Hahn, and K. Botzenhart, Transport of microorganisms in the underground: Processes, experiments, and simulation models, *Water Sci. Technol*., *24*(2), 309–314, 1991.

Thompson, S. S., and M. V. Yates, Bacteriophage inactivation at the air-water-solid interface in dynamic batch systems, *Appl. Environ. Microbiol*., *65*, 1186–1190, 1999.

Thompson, S. S., M. Flury, M. V. Yates, and W. A. Jury, Role of air-water interface in bacteriophage sorption experiments, *Appl. Environ. Microbiol*., *64*, 304–309, 1998.

Tim, U. S., and S. Mostaghimi, Model for predicting virus movement through soils, *Ground Water*, *29*(2), 251–259, 1991.

Trouwborst, T., S. Kuyper, and J. C. de Jong, Inactivation of some bacterial and animal viruses by exposure to liquid-air interfaces, *J. Gen. Virol*., *24*, 155–165, 1974.

van Genuchten, M. T., A closed form equation for predicting the hydraulic conductivity of unsaturated soils, *Soil Sci. Soc. Am. J*., *44*(5), 892–898, 1980.

Vilker, V. L., Simulating virus movement in soils, in *Modeling Waste Renovation: Land Treatment*, edited by I. K. Iskandar, pp. 223–253, John Wiley, New York, 1981.

Vilker, V. L., and W. D. Burge, Adsorption mass transfer model for virus transfer in soils, *Water Res*., *14*, 783–790, 1980.

Wan, J., and J. L. Wilson, Visualization of the role of the gas-water interface on the fate and transport of colloids in porous media, *Water Resour. Res*., *30*(1), 11–23, 1994a.

Wan, J., and J. L. Wilson, Colloid transport in unsaturated porous media, *Water Resour. Res*., *30*(4), 857–864, 1994b.

Yates, M. V., and Y. Ouyang, VIRTUS, a model of virus transport in unsaturated soils, *Appl. Environ. Microbiol*., *58*, 1609–1616, 1992.

Yates, M. V., and S. R. Yates, Modeling microbial fate in the subsurface environment, *Crit. Rev. Environ. Control*, *17*(4), 307–344, 1988.

C. V. Chrysikopoulos and Y. Sim, Department of Civil and Environmental Engineering, University of California, Irvine, ET844C Engineering Tower, Irvine, CA 92697-2175. (costas@eng.uci.edu)

(Received May 7, 1999; revised September 21, 1999;
accepted October 8, 1999.)